NOTES AND CORRESPONDENCE

Parameterization of the Optical Properties for Water Clouds in the Infrared

T. H. LINDNER AND J. LI

Canadian Centre for Climate Modelling and Analysis, Atmospheric Environment Service, University of Victoria, Victoria, British Columbia, Canada

9 April 1999 and 13 November 1999

ABSTRACT

A parameterization is presented for the optical properties of water clouds in the infrared spectrum. The cloud optical properties are parameterized in terms of the cloud's liquid water content and the effective radius defined from the droplet size distribution. Rational functions are used for the parameterization. The coefficients for the rational functions are derived by doing least square fitting to points calculated by exact Mie theory. The optical properties are presented for 36 individual wavelengths. Also, parameterizations in 12 spectral bands between 4 and 1000 μm are shown. The parameterization is valid for effective radius between 2 and 40 μm. The accuracy of the parameterization is mostly within 5% compared to the exact Mie calculations.

1. Introduction

For infrared radiation the scattering process is often neglected in climate models, since it is commonly believed that the scattering effect is small for the infrared. However, recent studies show that the infrared scattering by the cloud droplets could not be neglected in cloud cooling rates and surface radiation fluxes (Edwards and Slingo 1996). The reason for neglecting infrared scattering in climate models is that the scattering would make the calculation process much more complicated and dramatically increase the model's computing time. This problem recently has been solved by Li and Fu (2000). Since scattering of infrared radiation does not occur in cloud-free layers, it would be beneficial to find a way to account for scattering in cloud layers only. The method proposed by Li and Fu (2000) avoids the scattering calculation in cloud free layers and is therefore computationally efficient.

If scattering is neglected in the infrared (referred to as the absorption approximation), the only cloud optical property needed in the radiative transfer calculation is the absorption coefficient. To avoid the complicated Mie calculation, a parameterization of the absorption coefficient in terms of physical quantities that can be generated in climate models is needed. Chýlek and Ramaswamy (1982) proposed a simple parameterization of the emittance for water clouds in the infrared. A more sophisticated scheme was proposed by Chýlek et al. (1992). If scattering is considered in the infrared, more optical properties, such as the single-scattering albedo and the asymmetry factor, are needed. Also, only the parameterization for single wavelengths is considered in the previous works. The conversion to band results has not been discussed.

Hu and Stamnes (1993) is the only work that gives a parameterization of cloud optical properties in the infrared with scattering effects considered. The differences between this work and that of Hu and Stamnes (1993) are threefold. First, the wavelengths chosen match with those of the parameterization for ice cloud in Fu et al. (1998). This makes it simple to generate a complete parameterization for both water and ice clouds. Second in Hu and Stamnes (1993) exponential functions are used to parameterize the cloud's optical properties in terms of their effective radius. Exponential functions are computationally expensive and it is therefore preferable to avoid their use in GCMs. We will show that our parameterizations, based on rational functions, approximate well the exact Mie results while maintaining computational efficiency. Finally, in Hu and Stamnes (1993), the parameterizations are for three separate ranges of effective radius. In this work, a single parameterization covers effective radius from 2 to 40 μm.

2. Theory and parameterization

There are at least three relevant cloud optical properties that are needed in the radiative transfer process

Corresponding author address: Dr. Jiangnan Li, Canadian Centre for Climate Modelling and Analysis, Atmospheric Environment Service, P.O. Box 1700, University of Victoria, Victoria, BC V8P 2Y2, Canada.
E-mail: Jiangnan.Li@ec.gc.ca

if scattering is to be considered. They are the extinction coefficient, the single-scattering albedo, and the asymmetry factor. The extinction coefficient, k_{ext}^{λ}, for wavelength λ is defined as

$$k_{\text{ext}}^{\lambda} = \pi \int_0^{\infty} r^2 Q_{\text{ext}}(\lambda, r) n(r)\, dr, \tag{1}$$

where r is the droplet size, $n(r)$ is the distribution of droplet sizes, and Q_{ext} is the efficiency for the droplet to scatter plus absorb radiation.

The single-scattering albedo for wavelength λ, ω_{λ}, is the probability that a photon will survive a scattering event as opposed to being absorbed and is defined as

$$\omega_{\lambda} = \frac{\int_0^{\infty} r^2 Q_{\text{sca}}(\lambda, r) n(r)\, dr}{\int_0^{\infty} r^2 Q_{\text{ext}}(\lambda, r) n(r)\, dr}, \tag{2}$$

where Q_{sca} is the scattering efficiency.

The phase function, P, describes the angular distribution of scattered photons for scattering events. The normalized phase function for wavelength λ is given by

$$P(\theta, \lambda) = \frac{\dfrac{\lambda^2}{2\pi^2} \displaystyle\int_0^{\infty} [i_1(\theta, r, \lambda) + i_2(\theta, r, \lambda)] n(r)\, dr}{\displaystyle\int_0^{\infty} r^2 Q_{\text{sca}}(\lambda, r) n(r)\, dr}, \tag{3}$$

where θ is the scattering angle, and i_1 and i_2 are the squares of the vertical and horizontal scattering amplitudes (Bohren and Huffman 1983), respectively. Most radiative transfer methods require various moments of the Legendre expansion of the phase function. For example, the two-stream approximation requires the asymmetry factor g_{λ}, which is one-third of the first moment of the Legendre expansion of the phase function. All of the optical properties parameterized here (Q_{ext}, Q_{sca}, P, etc.) are obtained from Mie calculations.

The size distribution of cloud droplets in the atmosphere tend to closely resemble gamma distributions, which has the following form:

$$n(r) = Ar^{\alpha} e^{-\beta r}, \tag{4}$$

where A, α, and β are constants, and r is the radius of the cloud particle. The effective radius and the effective variance for a gamma distribution are given by

$$r_{\text{e}} = \frac{\int_0^{\infty} r^3 n(r)\, dr}{\int_0^{\infty} r^2 n(r)\, dr} = \frac{\alpha + 3}{\beta}, \quad \text{and} \tag{5}$$

$$\upsilon_{\text{e}} = \frac{\int_0^{\infty} (r - r_{\text{e}})^2 r^2 n(r)\, dr}{r_{\text{e}}^2 \int_0^{\infty} r^2 n(r)\, dr} = \frac{1}{\alpha + 3}. \tag{6}$$

There will not be any dependence on effective variance in our parameterization. Observations showed that υ_{e} varies little (Chýlek and Ramaswamy 1982) and that the variations that do occur are not very significant when calculating the optical properties. It is therefore reasonable to use a constant value of $\upsilon_{\text{e}} = 0.172$ in the Mie calculations (Dobbie et al. 1999). The constants of α and β in Eq. (4) can be defined by r_{e} and υ_{e} through Eqs. (5) and (6).

Usually, the extinction coefficient is normalized by dividing by the liquid water content. This gives $\psi_{\lambda} = k_{\text{ext}}^{\lambda}/\text{LWC}$, where ψ_{λ} is the specific extinction, and LWC is the liquid water content for the cloud. Since LWC is proportional to A in the gamma distribution, A is canceled out in the calculation of ψ_{λ}.

In Mie calculations for cloud optical properties, the refractive indices of water are taken from Hale and Querry (1984) and Downing and Williams (1975), and supplemented by Kou et al. (1993).

The integration to phase function in Legendre expansion to generate g_{λ} is performed at an angular resolution of 0.5°. A resolution of 0.05 μm is used for the droplet radius in calculations in Eqs. (1)–(3). We use simple rational functions to parameterize the cloud optical properties:

$$\psi_{\lambda} = a_0 + a_1 r_{\text{e}} + a_2/r_{\text{e}} + a_3/r_{\text{e}}^2 + a_4/r_{\text{e}}^3, \tag{7}$$

$$1 - \omega_{\lambda} = b_0 + b_1/r_{\text{e}} + b_2 r_{\text{e}} + b_3 r_{\text{e}}^2, \tag{8}$$

$$g_{\lambda} = c_0 + c_1/r_{\text{e}} + c_2 r_{\text{e}} + c_3 r_{\text{e}}^2. \tag{9}$$

The coefficients are derived from least squares fitting to the Mie calculation values. Given the nature of the least squares fitting it should be noted that our parameterization is meant to be valid for effective radius in the region 2–40 μm. The single-scattering coalbedo, $1 - \omega_{\lambda}$, is parameterized instead of the single-scattering albedo.

If we use a function $y_a(x; c_1, c_2, \ldots, c_M)$ to fit a curve $y(x)$, where $c_1, c_2, \ldots, c_M$ are M adjustable parameters, and we fit N data points $(x_i, y(x_i))$, $i = 1, 2, \ldots, N$, the least square fitting process is to minimize the value of

$$\sum_{i=1}^{N} [y(x_i) - y_a(x_i; c_1, c_2, \ldots, c_M)]^2$$

by choosing the suitable parameters $c_1, c_2, \ldots, c_M$

TABLE 1. Values of coefficients for the ψ_λ and ψ^i_{band} parameterizations.

	a_0 ($m^2\ g^{-1}$)	a_1 ($\mu m^{-1}\ m^2\ g^{-1}$)	a_2 ($\mu m\ m^2\ g^{-1}$)	a_3 ($\mu m^2\ m^2\ g^{-1}$)	a_4 ($\mu m^3\ m^2\ g^{-1}$)	Errors (%)
Wavelength (μm)						
4.000	-0.51604×10^{-2}	0.50969×10^{-3}	0.12213×10^{1}	0.74791×10^{1}	-0.13913×10^{2}	0.89%
4.566	-0.92239×10^{-1}	0.20047×10^{-2}	0.26616×10^{1}	0.74444	-0.69578×10^{1}	3.37%
5.000	−0.14408	0.28714×10^{-2}	0.35551×10^{1}	-0.36138×10^{1}	-0.21408×10^{1}	4.65%
6.061	−0.10481	0.19818×10^{-2}	0.33118×10^{1}	-0.65308×10^{1}	0.40348×10^{1}	1.70%
7.042	−0.21444	0.37715×10^{-2}	0.52442×10^{1}	-0.14991×10^{2}	0.12781×10^{2}	3.92%
8.065	−0.18232	0.29897×10^{-2}	0.51277×10^{1}	-0.17231×10^{2}	0.16837×10^{2}	2.06%
9.091	-0.89848×10^{-1}	0.12453×10^{-2}	0.39584×10^{1}	-0.14752×10^{2}	0.15449×10^{2}	3.00%
10.000	0.14532×10^{-1}	-0.47449×10^{3}	0.22898×10^{1}	-0.92402×10^{1}	0.100999×10^{2}	4.41%
10.989	0.45685×10^{-1}	-0.65270×10^{3}	0.12318×10^{1}	-0.45237×10^{1}	0.47859×10^{1}	2.73%
12.195	0.66177×10^{-3}	0.16683×10^{3}	0.17201×10^{1}	-0.47021×10^{1}	0.43364×10^{1}	1.29%
12.987	-0.17089×10^{-1}	0.45236×10^{-3}	0.20415×10^{1}	-0.51323×10^{1}	0.44923×10^{1}	0.92%
14.085	-0.32640×10^{-1}	0.69493×10^{-3}	0.23545×10^{1}	-0.57804×10^{1}	0.49161×10^{1}	0.68%
15.152	-0.44226×10^{-1}	0.87218×10^{-3}	0.25977×10^{1}	-0.64686×10^{1}	0.54707×10^{1}	0.55%
16.129	-0.51150×10^{-1}	0.97581×10^{-3}	0.27513×10^{1}	-0.69981×10^{1}	0.59455×10^{1}	0.49%
17.241	-0.57848×10^{-1}	0.10700×10^{-2}	0.29135×10^{1}	-0.77003×10^{1}	0.66516×10^{1}	0.49%
18.182	-0.61235×10^{1}	0.11091×10^{-2}	0.30169×10^{1}	-0.82877×10^{1}	0.73094×10^{1}	0.55%
19.231	-0.63215×10^{-1}	0.11209×10^{-2}	0.31052×10^{1}	-0.89067×10^{1}	0.80523×10^{1}	0.66%
20.000	-0.63149×10^{-1}	0.11033×10^{-2}	0.31461×10^{1}	-0.93069×10^{1}	0.85701×10^{1}	0.77%
20.833	-0.61903×10^{-1}	0.10638×10^{-2}	0.31723×10^{1}	-0.96949×10^{1}	0.91035×10^{1}	0.93%
22.222	-0.56709×10^{-1}	0.94835×10^{-3}	0.31596×10^{1}	-0.10123×10^{2}	0.97820×10^{1}	1.22%
22.727	-0.53573×10^{-1}	0.88640×10^{-3}	0.31329×10^{1}	-0.10200×10^{2}	0.99527×10^{1}	1.35%
23.810	-0.46845×10^{-1}	0.75468×10^{-3}	0.30734×10^{1}	-0.10326×10^{2}	0.10267×10^{2}	1.63%
25.641	-0.31854×10^{-1}	0.47647×10^{-3}	0.29056×10^{1}	-0.10258×10^{2}	0.10498×10^{2}	2.12%
26.316	-0.25513×10^{-1}	0.36207×10^{-3}	0.28276×10^{1}	-0.10158×10^{2}	0.10499×10^{2}	2.31%
29.412	0.64249×10^{-2}	-0.18480×10^{-3}	0.23803×10^{1}	-0.91730×10^{1}	0.98489×10^{1}	3.08%
31.250	0.25266×10^{-1}	-0.48259×10^{-3}	0.20737×10^{1}	-0.82700×10^{1}	0.90360×10^{1}	3.37%
34.483	0.46765×10^{-1}	-0.79241×10^{-3}	0.16806×10^{1}	-0.69737×10^{1}	0.77696×10^{1}	3.54%
38.462	0.62286×10^{-1}	-0.98558×10^{-3}	0.13509×10^{1}	-0.57934×10^{1}	0.65569×10^{1}	3.51%
43.478	0.65832×10^{-1}	-0.98550×10^{-3}	0.12094×10^{1}	-0.51671×10^{1}	0.58542×10^{1}	3.30%
47.619	0.67486×10^{-1}	-0.10158×10^{-2}	0.12161×10^{1}	-0.52456×10^{1}	0.59754×10^{1}	3.39%
50.000	0.71679×10^{-1}	-0.10923×10^{-2}	0.11831×10^{-1}	-0.52189×10^{1}	0.60019×10^{1}	3.54%
55.556	0.89700×10^{-1}	-0.14023×10^{-2}	0.96992	-0.47284×10^{1}	0.56474×10^{1}	4.03%
58.824	0.10451	-0.16478×10^{-2}	0.76704	-0.41622×10^{1}	0.51463×10^{1}	4.36%
66.667	0.14370	-0.22358×10^{-2}	0.11861	-0.20169×10^{1}	0.29910×10^{1}	4.81%
76.923	0.17729	-0.26324×10^{-2}	−0.58108	0.60431	0.15417	4.50%
100.00	0.17992	-0.21889×10^{-2}	-0.12545×10^{1}	0.36865×10^{1}	-0.35037×10^{1}	2.55%
Band No. / Band limits (μm)						
1 4.545–5.263	−0.14037E+00	0.28058E−02	0.34969E+01	−0.33770E+01	−0.23541E+01	4.52%
2 5.263–5.882	−0.20420E+00	0.37167E−02	0.48566E+01	−0.11972E+02	0.86344E+01	4.69%
3 5.882–7.143	−0.18318E+00	0.33080E−02	0.46120E+01	−0.11550E+02	0.87086E+01	3.65%
4 7.143–8.000	−0.20398E+00	0.34708E−02	0.52858E+01	−0.16603E+02	0.15392E+02	2.83%
5 8.000–9.091	−0.14269E+00	0.22282E−02	0.46478E+01	−0.16369E+02	0.16533E+02	1.73%
6 9.091–10.204	−0.24901E−01	0.16195E−03	0.29375E+02	−0.11437E+02	0.12273E+02	3.93%
7 10.204–12.500	0.29022E−01	−0.39657E−03	0.14902E+01	−0.50777E+01	0.52170E+01	2.51%
8 12.500–14.925	−0.23627E−01	0.55291E−03	0.21785E+01	−0.54664E+01	0.47379E+01	0.82%
9 14.925–18.519	−0.53069E−01	0.99992E−03	0.28045E+01	−0.72836E+01	0.62573E+01	0.51%
10 18.519–25.000	−0.57709E−01	0.99071E−03	0.31118E+01	−0.95540E+01	0.90189E+01	1.02%
11 25.000–35.714	0.41307E−03	−0.59631E−04	0.24275E+01	−0.90838E+01	0.96069E+01	2.77%
12 35.714–10.000	0.88116E−01	−0.12857E−02	0.81658E+00	−0.39428E+01	0.46652E+01	3.48%

(Press et al. 1992). Consequently, we define percentage error as

$$\frac{1}{N}\sum_{i=1}^{N}\frac{|y(x_i) - y_a(x_i; c_1, c_2, \ldots, c_M)|}{y(x_i)}100\%.$$

This is an averaged result for relative errors at N fitting points.

In our calculations, the variable x is the effective radius r_e and $y(r_e)$ represents the exact Mie calculated values. Here N is equal to 39, at an interval of 1 μm for r_e from 2 to 40 μm.

We present the parameterization for 36 individual wavelengths, the same as Fu et al. (1988). Coefficients for Eqs. (7)–(9) are presented in Tables 1–3 along with the percentage error for each wavelength.

We also present the band-averaged results, and fitting

TABLE 2. Values of coefficients for the $(1 - \omega_\lambda)$ and $(1 - \omega^i_{\text{band}}$ parameterizations.

Wavelengths (μm)	b_0	b_1 (μm)	b_2 (μm^{-1})	b_3 (μm^{-2})	Errors (%)
4.000	-0.23193×10^{-2}	0.17819×10^{-2}	0.12942×10^{-1}	-0.15693×10^{-3}	2.50%
4.566	0.42346×10^{-1}	-0.16581×10^{-1}	0.21225×10^{-1}	-0.30668×10^{-3}	3.80%
5.000	0.40076×10^{-3}	0.71639×10^{-1}	0.21413×10^{-1}	-0.30024×10^{-3}	3.38%
6.061	0.37537	0.32545	0.84345×10^{-2}	-0.15020×10^{-3}	1.48%
7.042	0.51758×10^{-2}	0.41035	0.27486×10^{-1}	-0.41800×10^{-3}	2.79%
8.065	-0.46028×10^{-1}	0.66826	0.27724×10^{-1}	-0.39535×10^{-3}	1.57%
9.091	-0.29070×10^{-1}	0.91717	0.24274×10^{-1}	-0.31609×10^{-3}	1.03%
10.000	0.10281	0.10623×10^{1}	0.14751×10^{-1}	-0.15273×10^{-3}	1.30%
10.989	0.49046	0.78525	-0.42690×10^{-2}	0.10571×10^{-3}	1.45%
12.195	0.64862	0.56208	-0.94341×10^{-2}	0.15079×10^{-3}	0.97%
12.987	0.62342	0.58170	-0.82567×10^{-2}	0.13037×10^{-3}	0.86%
14.085	0.59208	0.61011	-0.66103×10^{-2}	0.10374×10^{-3}	0.72%
15.152	0.56899	0.63277	-0.52584×10^{-2}	0.81771×10^{-4}	0.61%
16.129	0.55705	0.64877	-0.45221×10^{-2}	0.69635×10^{-4}	0.55%
17.241	0.54294	0.67056	-0.36174×10^{-2}	0.55117×10^{-4}	0.49%
18.182	0.53274	0.69120	-0.29499×10^{-2}	0.44807×10^{-4}	0.46%
19.231	0.52211	0.71607	-0.22650×10^{-2}	0.34605×10^{-4}	0.45%
20.000	0.51518	0.73516	-0.18318×10^{-2}	0.28505×10^{-4}	0.46%
20.833	0.50769	0.75692	-0.13829×10^{-2}	0.22483×10^{-4}	0.48%
22.222	0.49939	0.79025	-0.93583×10^{-3}	0.17637×10^{-4}	0.54%
22.727	0.49783	0.80139	-0.87766×10^{-3}	0.17731×10^{-4}	0.58%
23.810	0.49428	0.82428	-0.75616×10^{-3}	0.17976×10^{-4}	0.65%
25.641	0.49162	0.85875	-0.82652×10^{-3}	0.23453×10^{-4}	0.79%
26.316	0.49135	0.87014	-0.91834×10^{-3}	0.26691×10^{-4}	0.86%
29.412	0.50596	0.89577	-0.23286×10^{-2}	0.56852×10^{-4}	1.16%
31.250	0.53079	0.88214	-0.40583×10^{-2}	0.87518×10^{-4}	1.35%
34.483	0.58768	0.82164	-0.74467×10^{-2}	0.14173×10^{-3}	1.56%
38.462	0.65905	0.72632	-0.11260×10^{-1}	0.19852×10^{-3}	1.71%
43.478	0.74095	0.59872	-0.15013×10^{-1}	0.24845×10^{-3}	1.73%
47.619	0.76761	0.55924	-0.16237×10^{-1}	0.26447×10^{-3}	1.76%
50.000	0.77424	0.55231	-0.16651×10^{-1}	0.27101×10^{-3}	1.81%
55.556	0.78131	0.55198	-0.17410×10^{-1}	0.28589×10^{-3}	1.97%
58.824	0.78200	0.55847	-0.17786×10^{-1}	0.29494×10^{-3}	2.09%
66.667	0.79548	0.55203	-0.19436×10^{-1}	0.32962×10^{-3}	2.41%
76.923	0.83677	0.49254	-0.22706×10^{-1}	0.38832×10^{-3}	2.74%
100.00	0.96729	0.25810	-0.31074×10^{-1}	0.51700×10^{-3}	2.98%
Band No.	Band limits (μm)				
1	4.545–5.263	0.68056E−02	0.59837E−01	0.21125E−01	−0.29740E−03	3.41%
2	5.263–5.882	−0.14764E−01	0.28331E+00	0.23515E−01	−0.33662E−03	2.45%
3	5.882–7.143	0.11595E+00	0.30559E+00	0.22727E−01	−0.36032E−03	2.78%
4	7.143–8.000	−0.27033E−01	0.54717E+00	0.27903E−01	−0.41074E−03	2.11%
5	8.000–9.091	−0.43354E−01	0.78454E+00	0.26449E−01	−0.36385E−03	1.20%
6	9.091–10.204	0.46323E−01	0.10131E+01	0.18692E−01	−0.21898E−03	1.08%
7	10.204–12.500	0.49787E+00	0.74581E+00	−0.37379E−02	0.90555E−04	1.25%
8	12.500–14.925	0.60890E+00	0.59525E+00	−0.74557E−02	0.11757E−03	0.79%
9	14.925–18.519	0.55180E+00	0.65812E+00	−0.41768E−02	0.64243E−04	0.53%
10	18.519–25.000	0.50964E+00	0.76057E+00	−0.15630E−02	0.26245E−04	0.52%
11	25.000–35.714	0.51897E+00	0.86352E+00	−0.29099E−02	0.63126E−04	1.11%
12	35.714–10.000	0.76110E+00	0.57048E+00	−0.16721E−01	0.27886E−03	1.91%

is done for 12 bands. The calculations are based on 203 wavelengths ranging from 4 to 1000 μm. The parameterization formulas are the same as Eqs. (7)–(9).

For solar radiation, the weights for each individual wavelength in a band are based on the solar spectrum at the top of the atmosphere. Li et al. (1997) pointed out that, for water clouds, the solar spectrum at the top of the cloud should be significantly different from that at the top of the atmosphere. The cloud heating rate will be largely affected by using different solar spectral weights. The solar spectral weight at 700 mb has been used in Dobbie et al. (1999) for a new proposed parameterization of cloud optical properties for solar radiation. For the infrared, the downward radiative flux at a cloud top depends on the emission and attenuation of radiation from all layers above the cloud layer, and the upward radiative flux at the bottom of the cloud layer depends on the emission and attenuation of radiation from all layers below the cloud layer. However, in both cases, the layers adjacent to the cloud layer have the biggest influence, because the cloud receives the blackbody emission from these layers without gaseous attenuation.

TABLE 3. Values of coefficients for the g_λ and g^i_{band} parameterizations.

Wavelengths (μm)	c_0	c_1 (μm)	c_2 (μm^{-1})	c_3 (μm^{-2})	Errors (%)
4.000	0.71900	0.14112	0.90171×10^{-2}	-0.11494×10^{-3}	0.55%
4.566	0.78868	0.15719×10^{-2}	0.70250×10^{-2}	-0.78742×10^{-4}	0.66%
5.000	0.81140	-0.59356×10^{-1}	0.45315×10^{-2}	-0.32407×10^{-4}	0.86%
6.061	0.99274	−0.51551	-0.64373×10^{-3}	0.89127×10^{-5}	0.16%
7.042	0.93222	−0.46655	-0.94508×10^{-3}	0.48750×10^{-4}	0.81%
8.065	0.99511	−0.68602	-0.47012×10^{-2}	0.1046×10^{-3}	0.70%
9.091	0.10445×10^{1}	−0.89730	-0.61798×10^{-2}	0.11314×10^{-3}	0.45%
10.000	0.10717×10^{1}	-0.10639×10^{1}	-0.56000×10^{-2}	0.87940×10^{-4}	0.27%
10.989	0.10841×10^{1}	-0.12213×10^{1}	-0.43931×10^{-2}	0.60716×10^{-4}	0.19%
12.195	0.10604×10^{1}	-0.13289×10^{1}	-0.30423×10^{-2}	0.36010×10^{-4}	0.19%
12.987	0.10344×10^{1}	-0.13581×10^{1}	-0.20294×10^{-2}	0.18643×10^{-4}	0.26%
14.085	0.10034×10^{1}	-0.13829×10^{1}	-0.68814×10^{-3}	-0.38752×10^{-5}	0.44%
15.152	0.97455	-0.13959×10^{1}	0.67707×10^{-3}	-0.26408×10^{-4}	0.63%
16.129	0.94859	-0.14040×10^{1}	0.19908×10^{-2}	-0.48011×10^{-4}	0.82%
17.241	0.91927	-0.14044×10^{1}	0.35145×10^{-2}	-0.72656×10^{-4}	1.03%
18.182	0.89561	-0.14020×10^{1}	0.47867×10^{-2}	-0.92998×10^{-4}	1.22%
19.231	0.86967	-0.13957×10^{1}	0.61874×10^{-2}	-0.11514×10^{-3}	1.42%
20.000	0.85122	-0.13899×10^{1}	0.71901×10^{-2}	-0.13085×10^{-3}	1.58%
20.833	0.83164	-0.13822×10^{1}	0.82480×10^{-2}	-0.14726×10^{-3}	1.74%
22.222	0.79950	-0.13674×10^{1}	0.99854×10^{-2}	-0.17415×10^{-3}	2.03%
22.727	0.78828	-0.13622×10^{1}	0.10602×10^{-1}	-0.18370×10^{-3}	2.14%
23.810	0.76366	-0.13475×10^{1}	0.11919×10^{-1}	-0.20396×10^{-3}	2.39%
25.641	0.72330	-0.13199×10^{1}	0.14071×10^{-1}	-0.23689×10^{-3}	2.83%
26.316	0.70872	-0.13087×10^{1}	0.14841×10^{-1}	-0.24863×10^{-3}	3.00%
29.412	0.64127	-0.12491×10^{1}	0.18458×10^{-1}	-0.30450×10^{-3}	3.87%
31.250	0.59931	-0.12059×10^{1}	0.20814×10^{-1}	-0.34180×10^{-3}	4.48%
34.483	0.51851	-0.11038×10^{1}	0.25244×10^{-1}	-0.41142×10^{-3}	5.56%
38.462	0.41774	−0.95601	0.30507×10^{-1}	-0.49188×10^{-3}	6.75%
43.478	0.29104	−0.74514	0.36469×10^{-1}	-0.57810×10^{-3}	7.79%
47.619	0.20494	−0.58594	0.39479×10^{-1}	-0.61470×10^{-3}	8.00%
50.000	0.16538	−0.50925	0.40523×10^{-1}	-0.62429×10^{-3}	7.97%
55.556	0.96580×10^{-1}	−0.37029	0.41594×10^{-1}	-0.62513×10^{-3}	7.62%
58.824	0.69419×10^{-1}	−0.31256	0.41503×10^{-1}	-0.61482×10^{-3}	7.35%
66.667	0.27115×10^{-1}	−0.22243	0.40642×10^{-1}	-0.58495×10^{-3}	7.09%
76.923	-0.13640×10^{-1}	−0.13593	0.39433×10^{-1}	-0.55179×10^{-3}	7.10%
100.00	-0.87501×10^{-1}	-0.21285×10^{-1}	0.38102×10^{-1}	-0.51750×10^{-3}	6.77%
Band No.	Band limits (μm)				
1	4.545–5.263	0.81237E+00	−0.59116E−01	0.45815E−02	−0.34183E−04	0.83%
2	5.263–5.882	0.91157E+00	−0.28177E+00	−0.76141E−03	0.48507E−04	0.85%
3	5.882–7.143	0.92873E+00	−0.42761E+00	0.59324E−03	0.13310E−04	0.59%
4	7.143–8.000	0.96560E+00	−0.58093E+00	−0.30781E−02	0.81913E−04	0.78%
5	8.000–9.091	0.10191E+01	−0.78499E+00	−0.55350E−02	0.11148E−03	0.58%
6	9.091–10.204	0.10622E+01	−0.10022E+01	−0.58929E−02	0.98522E−04	0.33%
7	10.204–12.500	0.10762E+01	−0.12381E+01	−0.41201E−02	0.56101E−04	0.16%
8	12.500–14.925	0.10198E+01	−0.13674E+01	−0.13742E−02	0.77369E−05	0.34%
9	14.925–18.519	0.93790E+00	−0.14017E+01	0.25612E−02	−0.57108E−04	0.89%
10	18.519–25.000	0.82701E+00	−0.13771E+01	0.84954E−02	−0.15092E−03	1.77%
11	25.000–35.714	0.64693E+00	−0.12450E+01	0.18208E−01	−0.30120E−03	3.68%
12	35.714–10.000	0.21512E+00	−0.57744E+00	0.35799E−01	−0.54520E−03	6.98%

Therefore we average the band results with respect to the Planck function. For example, the band-averaged value for the specific extinction is defined as

$$\psi^i_{\text{band}} = \int_{\Delta\lambda_i} \psi_\lambda B_\lambda(T)\, d\lambda \Big/ \int_{\Delta\lambda_i} B_\lambda(T)\, d\lambda, \quad (10)$$

where $B_\lambda(T)$ is the Planck function, T is the temperature, and $\Delta\lambda_i$ is the spectral interval for band i. Equation (10) is physically similar to the Chandraskhar mean (Liou 1992). The Chandraskhar mean requires a weighting by incoming radiative flux to the cloud. However, for the infrared the incoming radiative flux is not available till the radiative transfer process is performed.

We find that the band results of cloud infrared optical properties are not sensitive to the temperature for the Planck function. Figures 1a and 1b show the extent of the error that could be introduced by weighting the averages for each band by the Planck function with T at 180 and 320 K. The results for two bands are shown. Band 1 (4.54–5.26 μm) is at the beginning of the infrared spectrum with a small band weight in radiative

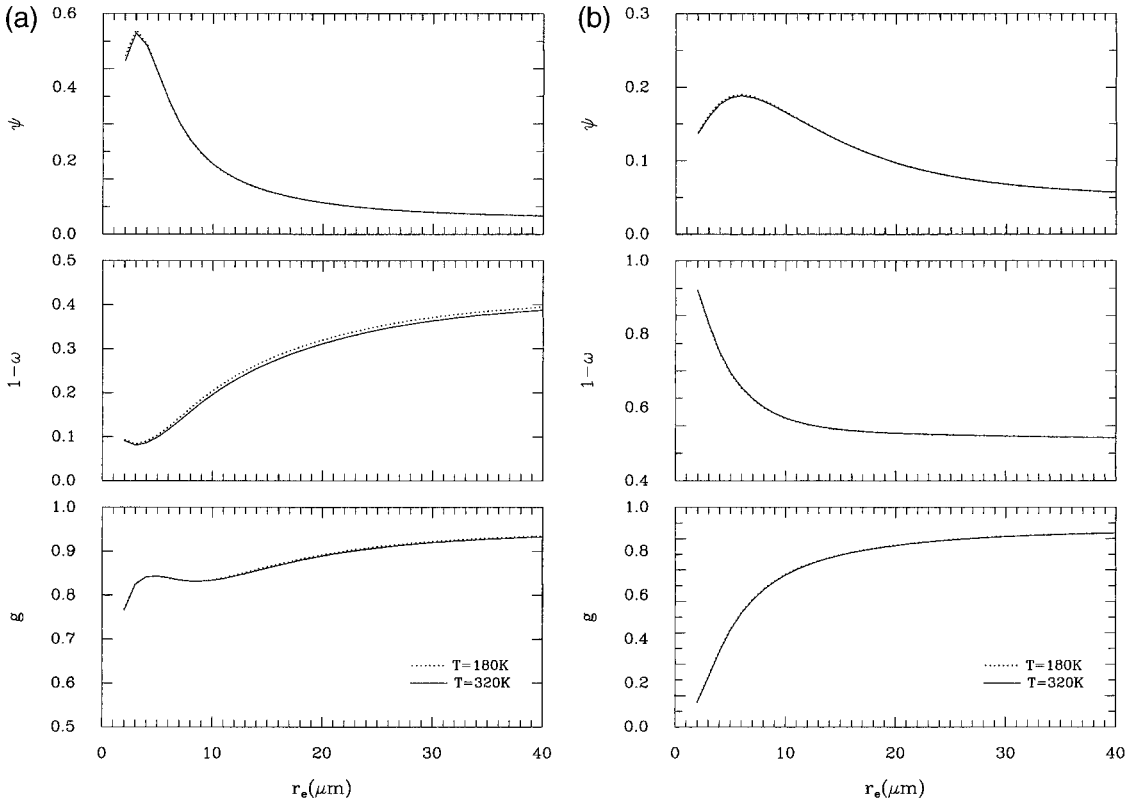

FIG. 1. (a) Comparison of the results of calculating the weighted average with the Planck function at $T = 180$ and 320 K. All three properties are plotted with respect to r_e. These are the results for spectral band 1 (4.54–5.26 μm). (b) As in (a), but for spectral band 11 (25.000–35.714 μm).

calculations. Band 11 (25.000–35.714 μm) is at the center of the infrared spectrum with a large band weight in radiative calculations. The error introduced by weighting at different temperatures is found to be very small for all bands. Given these small errors it appears that there is little dependence on temperature in our weighting. All band results are derived by weighting the average with the Planck function at 275 K.

Figures 2a–c show the differences between exact values for the single-scattering properties and the curves that are obtained from the parameterization. The results of bands 1, 5, and 11 are presented. It is found that ψ^i_{band}, ω^i_{band}, and g^i_{band} do not, in general, monotonically increase or decrease with the increase of r_e. The behavior of cloud optical properties are particularly complicated for effective radii less than 5 μm. However, the proposed simple parameterization scheme always approximates well the exact Mie results. Tables 1, 2, and 3 list the percentage error for the parameterizations for band-averaged results. It is found that errors are seldom greater than 5%.

For infrared radiation, if scattering is neglected the dominant process is absorptance. In the following we will show the validity of using averaged band optical properties in absorptance calculations. The absorptance for a single wavelength is

$$\text{Abs}_\lambda = 1 - e^{-(1-\omega_\lambda)k^\lambda_{\text{ext}}z} = 1 - e^{-(1-\omega_\lambda)\psi_\lambda \text{LWP}}, \quad (11)$$

where z is the cloud layer thickness and $(1 - \omega_\lambda)k^\lambda_{\text{ext}}$ is the absorption coefficient. The liquid water path, LWP, is defined as LWP = LWCz. Using our parameterization the absorptance for band i, $\overline{\text{Abs}}^i_{\text{band}}$, can be calculated as

$$\overline{\text{Abs}}^i_{\text{band}} = 1 - e^{-(1-\omega^i_{\text{band}})\psi^i_{\text{band}}\text{LWP}}, \quad (12)$$

where $1 - \omega^i_{\text{band}}$ and ψ^i_{band} are our weighted averages for a given spectral band i. The precise method would be to calculate the absorption for each wavelength first and then calculate the weighted averages of the absorption over the band, in the following way:

$$\text{Abs}^i_{\text{band}} = \frac{\int_{\Delta\lambda_i} 1 - e^{-(1-\omega_\lambda)\psi_\lambda \text{LWP}} B_\lambda(T)\, d\lambda}{\int_{\Delta\lambda_i} B_\lambda(T)\, d\lambda}. \quad (13)$$

The formulation for absorption in Eq. (13) is significantly more complicated than the one in Eg. (12). Figures 3a, 3b, and 3c (for bands 1, 5, and 11) show a comparison between absorption curves calculated using our parameterization and those using the formulation of Eq. (13) based on exact Mie calculation. The absorption

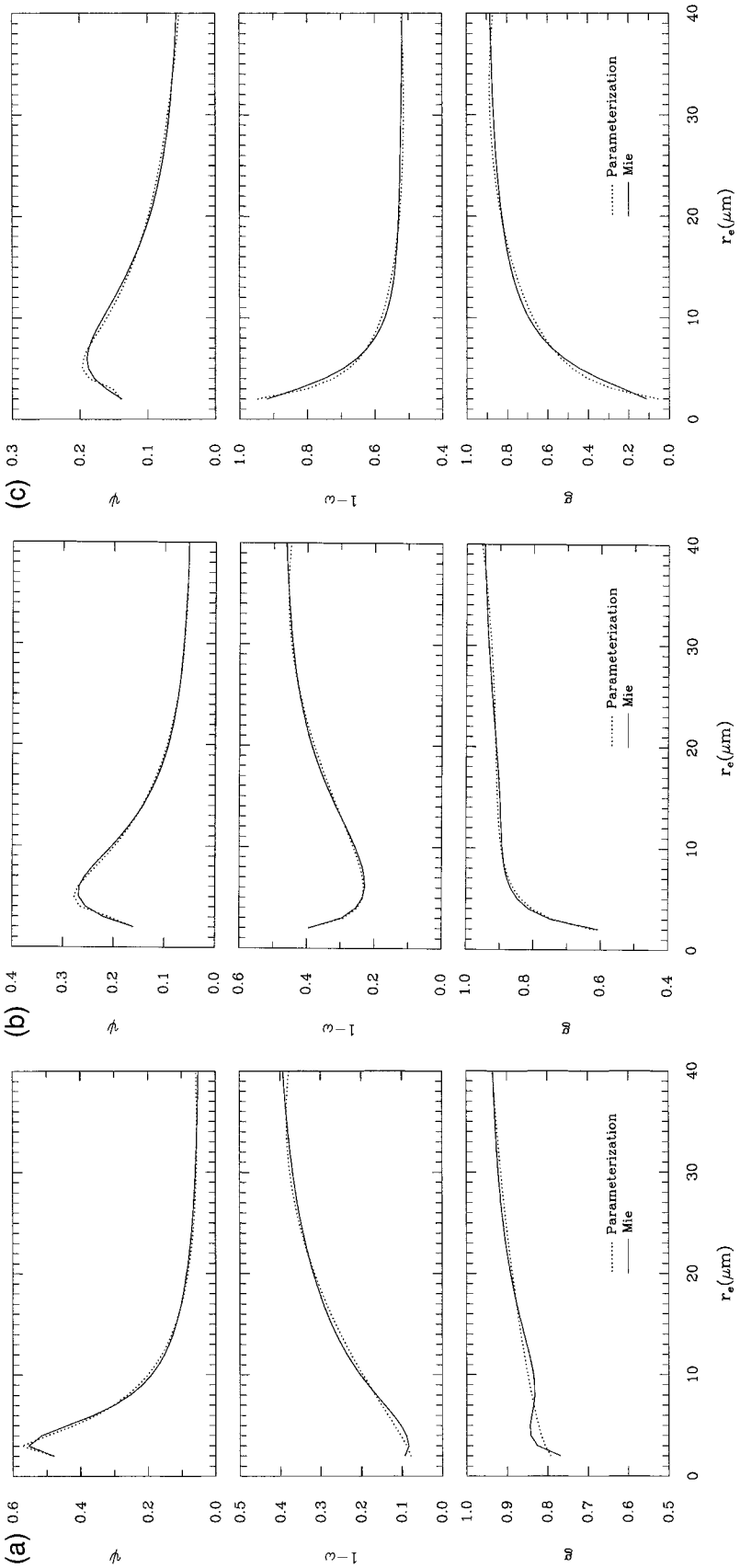

FIG. 2. (a) Comparison of the optical properties as derived by parameterization and by exact Mie calculations. All three properties are plotted with respect to r_e. These are the results for spectral band 1 (4.54–5.26 μm). (b) As in (a), but for spectral band 5 (8.000–9.091 μm). (c) As in (a), but for spectral band 11 (25.000–35.714 μm).

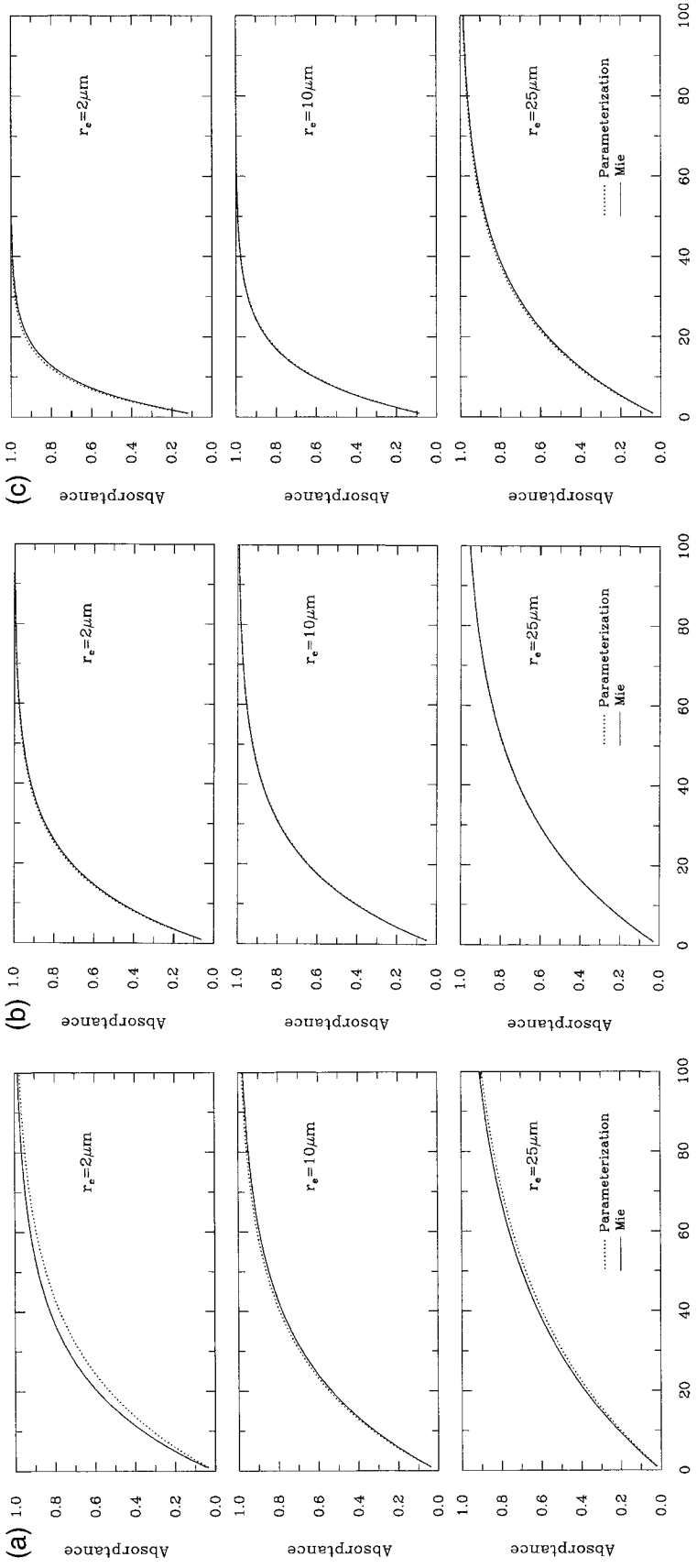

FIG. 3. (a) Comparison of band absorptance curves. The parameterized curve is the absorptance derived by using the extinction coefficient and single-scattering coalbedo for that band as in Eq. (12). The exact curve is the absorptance curve derived by using the more precise formulation of Eq. (13). Each of the graphs is defined for a given r_e. These are the results for spectral band 1 (4.54–5.26 μm). (b) As in (a), but for spectral band 5 (8.000–9.091 μm). (c) As in (a), but for spectral band 11 (25.000–35.714 μm).

curves are plotted versus the LWP. Here $r_e = 2$, 10, and 25 μm are considered. The figures demonstrate that the band parameterization always gives an accurate approximation of the absorption curve. The worst case occurs for band 1 with $r_e = 2$ μm, since in this case the errors for both ψ^i_{band} and ω^i_{band} are relatively large (see Tables 1 and 2).

3. Summary

This paper presents a parameterization of the optical properties of liquid water clouds for radiation in the infrared spectrum. The properties are parameterized in terms of the effective radius of their droplet size distribution and liquid water content. Parameterizations for 36 individual wavelengths in the infrared region are presented. Also, the results from the Mie calculations were averaged into 12 spectral bands. The parameterized curves approximate well the exact Mie values, with percentage errors mostly less than 5% for all the optical properties. Since Fu et al. (1998) has proposed a parameterization for ice cloud in the infrared, a corresponding parameterization for water clouds is necessary to define a complete parameterization for cloud optical properties in the infrared.

Acknowledgments. The authors would thank Drs. N. A. McFarlane and J. Scinoca and anonymous reviewers for their helpful comments.

REFERENCES

Bohren, C. F., and D. R. Huffman, 1983: *Absorption and Scattering of Light by Small Particles.* Wiley, 536 pp.

Chýlek, P., and V. Ramaswamy, 1982: Simple approximation for infrared emissivity of water clouds. *J. Atmos. Sci.,* **39,** 171–177.

——, P. Damiano, and E. P. Shettle, 1992: Infrared emittance of water clouds. *J. Atmos. Sci.,* **49,** 1459–1472.

Dobbie, J. S., J. Li, and P. Chýlek, 1999: Two and four stream optical properties for water clouds and solar wavelengths. *J. Geophys. Res.,* **104,** 2067–2079.

Downing, H. D., and D. Williams, 1975: Optical constants of water in the infrared. *J. Geophys. Res.,* **80,** 1656–1661.

Edwards, J. M., and A. Slingo, 1996: Studies with a flexible new radiation code. I: Choosing a configuration for a large-scale model. *Quart. J. Roy. Meteor. Soc.,* **122,** 689–719.

Fu, Q., P. Yang, and W. B. Sun, 1998: An accurate parameterization of the infrared radiative properties of cirrus clouds for climate models *J. Climate,* **11,** 2223–2237.

Hale, G., and M. Querry, 1984: Optical constants of water in the 200 *nm* to 200 μm wavelength region. *Appl. Opt.,* **23,** 1206–1225.

Hu, Y., and K. Stamnes, 1993: An accurate parameterization of the radiative properties of water clouds suitable for use in climate models. *J. Climate,* **6,** 728–742.

Kou, L., D. Labrie, and P. Chýlek, 1993: Refractive indices of water and ice in the 0.65–2.5μm spectral range. *Appl. Opt.,* **32,** 3531–3540.

Li, J., and Q. Fu, 2000: Absorption approximation with scattering effect for infrared radiation. *J. Atmos. Sci.,* in press.

——, S. M. Freidenreich, and V. Ramaswamy, 1997: Solar spectral weight at low cloud tops. *J. Geophys. Res.,* **102,** 11 139–11 143.

Liou, K.-N., 1992: *Radiative Transfer and Cloud Process in the Atmosphere.* Oxford University Press, 478 pp.

Press, W. H., S. A. Teukolsky, W. T. Vetterling and B. P. Flannery, 1992: *Numerical Recipies in Fortran 77.* Cambridge University Press, 933 pp.